

****Volume Title****

*ASP Conference Series, Vol. **Volume Number***

****Author****

© ****Copyright Year**** *Astronomical Society of the Pacific*

An anisotropic-Alfvénic-turbulence-based solar wind model with proton temperature anisotropy

Bo Li¹ and Shadia Rifai Habbal²

¹*Shandong Provincial Key Laboratory of Optical Astronomy & Solar-Terrestrial Environment, School of Space Science and Physics, Shandong University at Weihai, Weihai 264209, China*

²*Institute for Astronomy, University of Hawaii, 2680 Woodlawn Drive, Honolulu, HI 96822, USA*

Abstract. How the solar wind is accelerated to its supersonic speed is intimately related to how it is heated. Mechanisms based on ion-cyclotron resonance have been successful in explaining a large number of observations, those concerning the significant ion temperature anisotropy above coronal holes in particular. However, they suffer from the inconsistency with turbulence theory which says that the turbulent cascade in a low-beta medium like the solar corona should proceed in the perpendicular rather than the parallel direction, meaning that there is little energy in the ion gyro-frequency range for ions to absorb via ion-cyclotron resonance. Recently a mechanism based on the interaction between the solar wind particles and the anisotropic turbulence has been proposed, where the perpendicular proton energy addition is via the stochastic heating (Chandran et al. 2011). We extend this promising mechanism by properly accounting for the effect of proton temperature anisotropy on the propagation of Alfvén waves, for the radiative losses of electron energy, and for the field line curvature that naturally accompanies solar winds in the corona. While this mechanism was shown in previous studies to apply to the polar fast solar wind, we demonstrate here for the first time that it applies also to the slow wind flowing along field lines bordering streamer helmets.

1. Modeling the solar wind: why temperature anisotropy?

How the solar wind is accelerated is closely related to how it is heated (e.g., Cranmer 2009). For the nascent fast wind above coronal holes, much evidence exists that ions are hotter than electrons, and their perpendicular temperatures are higher than the parallel one ($T^\perp > T^\parallel$) (see data compiled in Cranmer 2002, also Cranmer et al. 2008). Interestingly, in the near-Sun region the slow wind flanking streamer helmets exhibits a similar tendency as evidenced by measurements with SOHO/UVCS (Strachan et al. 2002; Frazin et al. 2003). Given that the solar winds receive most acceleration close to the Sun, these observations point to the possibility that the fast and slow winds may share a common heating, and hence acceleration, mechanism. Some other factors, most notably the distinct flow tube geometry, then determine the heating profile and hence lead to significantly different terminal speeds of the two winds (Wang & Sheeley 1990; Cranmer et al. 2007).

The temperature measurements, especially the inferred significant ion temperature anisotropy, lead naturally to the suggestion that the nascent solar winds are heated

by ion-cyclotron resonance (e.g., Hollweg & Isenberg 2002). The needed high frequency ion-cyclotron waves (ICWs) may be generated either by a turbulent parallel cascade from low-frequency waves emitted by the Sun, or directly by small-scale magnetic reconnection events at chromospheric network. While the latter remains safe, the former has been challenged recently as both MHD turbulence theory and simulation studies (e.g., Cho et al. 2003) suggest that in a low- β solar corona, the turbulence cascade prefers the \perp -direction, hence generating modes with high k_{\perp} instead of ICWs with high k_{\parallel} and high frequency. However, these high- k_{\perp} modes, presumably kinetic Alfvén waves (KAWs), are most readily dissipated by electrons in a low- β plasma, if the only dissipation channel is via the Landau resonance. The consequent preferential electron heating would violate available measurements. A remedy comes only recently, where KAWs with sufficient amplitudes were demonstrated to primarily heat protons, preferentially in the \perp -direction, by rendering the ion orbits stochastic (Chandran et al. 2010). This nonlinear mechanism, termed “stochastic heating”, was further parameterized (Chandran 2010) and eventually incorporated into a two-fluid solar wind model (Chandran et al. 2011)(hereafter C11) where the anisotropic turbulence was shown to be capable of producing polar fast solar wind solutions that agree with a substantial number of observations.

Given that the fast and slow winds may share a common heating mechanism, and that C11 is restricted to the polar fast wind, we wish to extend C11 by asking whether the mechanism therein also applies to the equatorial slow wind as well. To address this, we construct slow wind models that are based on the anisotropic turbulence, that distinguish between electrons and protons, and that account for the proton temperature anisotropy. Inherited from C11 are: 1) The turbulence is driven by reflections of outward (z^+) waves off the gradients of the solar wind parameters, 2) Outward waves z^+ dominate inward ones z^- , 3) z^- waves are cascaded sufficiently fast compared with their wave periods, 4) the cascade proceeds in the inertial range along a “critical balance” path until it reaches a \perp -scale comparable to the ion gyroradius, where the generated KAWs are damped via both Landau damping (yielding electron heating, and proton \parallel -heating), and stochastic heating (yielding proton \perp -heating), 5) if the wave energy is cascaded to smaller still \perp -scales, only electrons receive this energy. However, compared with C11, we: 1) properly incorporate in the gross dissipation rate the field line curvature that accompanies field lines bordering streamer helmets, 2) incorporate the radiative loss in the electron energy equation, which is important in the energy balance in the upper transition region, 3) improve the treatment of wave propagation by including the effects of temperature anisotropy, which was missing in the original treatment in C11. For simplicity, instead of a more self-consistent, collisionless treatment of the proton heat fluxes based on the Landau fluid approach as was adopted by C11, we assume that the fluxes can be described by a modified Spitzer form. In what follows, we describe the improved model in section 2, present a constructed slow wind model in section 3, and summarize our effort in section 4.

2. Model description and method of solution

The fluid part of our model starts with the standard 16-moment transport equations (see appendix in Li & Li 2009). When axial symmetry is assumed and solar rotation neglected, in a steady state the vector equations may be decomposed into a force balance condition across the meridional magnetic field lines and a set of transport equations

along them. For simplicity we replace the former by prescribing a meridional magnetic field configuration presented in Banaszekiewicz et al. (1998), which is representative of a minimum corona. The transport equations along curved field lines then read

$$(nva)' = 0, \quad (1)$$

$$vv' + \frac{k_B}{nm_p} [n(T_p^{\parallel} + T_e)]' + \frac{k_B(T_p^{\parallel} - T_p^{\perp})a'}{am_p} - \left(\frac{GM_{\odot}}{r}\right)' - \frac{F}{nm_p} = 0, \quad (2)$$

$$v(T_e)' + \frac{(\gamma - 1)T_e(av)'}{a} - \frac{\gamma - 1}{nk_B a} (a\kappa_{e0}T_e^{5/2}T_e)'$$

$$+ 2v_{pe}(T_e - T_p) - \frac{\gamma - 1}{nk_B}(Q_e - L_{\text{rad}}) = 0, \quad (3)$$

$$v(T_p^{\parallel})' + 3(\gamma - 1)T_p^{\parallel}v' - \frac{\gamma - 1}{nk_B a} [a\tilde{\kappa}_{p0}T_p^{5/2}(T_p^{\parallel})']'$$

$$+ 2v_{pe}(T_p^{\parallel} - T_e) + 2v_{pp}(T_p^{\parallel} - T_p^{\perp}) - \frac{3(\gamma - 1)Q_p^{\parallel}}{nk_B} = 0, \quad (4)$$

$$v(T_p^{\perp})' + \frac{3(\gamma - 1)vT_p^{\perp}a'}{2a} - \frac{\gamma - 1}{nk_B a} [a\tilde{\kappa}_{p0}T_p^{5/2}(T_p^{\perp})']'$$

$$+ 2v_{pe}(T_p^{\perp} - T_e) + v_{pp}(T_p^{\perp} - T_p^{\parallel}) - \frac{3(\gamma - 1)Q_p^{\perp}}{2nk_B} = 0. \quad (5)$$

Here n is the number density and v the speed, $a \propto 1/B$ is the tube cross-sectional area with B being the magnetic field strength. An arbitrary point along a field line is characterized by both (r, θ) (its heliocentric distance and colatitude) and arclength l . The prime $'$ denotes the differentiation with respect to l . Moreover, k_B and m_p are the Boltzmann constant and proton mass. The gravitational constant is denoted by G , and solar mass by M_{\odot} . The electron, proton parallel and perpendicular temperatures are denoted by T_e , T_p^{\parallel} and T_p^{\perp} , respectively. The mean proton temperature is given by $T_p = (T_p^{\parallel} + 2T_p^{\perp})/3$. Furthermore, $\gamma = 5/3$ is the adiabatic index. The Coulomb collision rates v_{pe} and v_{pp} are evaluated by using a Coulomb logarithm of 23. For simplicity, the Spitzer law is assumed for the electron heat flux, $\kappa_{e0} = 7.8 \times 10^{-7}$ (cgs units will be used throughout). A similar form is assumed for the proton ones, but the coefficient is arbitrarily reduced relative to the Spitzer value $\kappa_{p,c} = 3.2 \times 10^{-8}$ by a spatially varying factor, namely, $\tilde{\kappa}_{p0}/\kappa_{p,c}$ is 1 for $r < 3 R_{\odot}$, ramped linearly with r to 0.02 at $r = 10 R_{\odot}$ and kept so from there on (see e.g., Li et al. 1999). Besides, L_{rad} represents the radiative losses and we adopt the standard parametrization by Rosner et al. (1978) for an optically thin medium. Q_e , Q_p^{\parallel} and Q_p^{\perp} are the heating rates, while F represents the volumetric force density the solar wind receives. Part of the electron heating is assumed to come from some ad hoc process which operates close to the base, $Q_{e,\text{basal}} = Q_{e0} \exp(-l/l_d)$. This basal heating is found to be important to improve the agreement of the model results with observations. On the other hand, the majority of the electron heating $Q_{e,\text{wav}}$, as well as the proton heating rates, are due entirely to the turbulent dissipation of low-frequency Alfvén waves.

The wave part of the model is a WKB evolution equation with dissipation terms,

$$\frac{(aF_w)'}{a} + vF = -Q_{\text{wav}}. \quad (6)$$

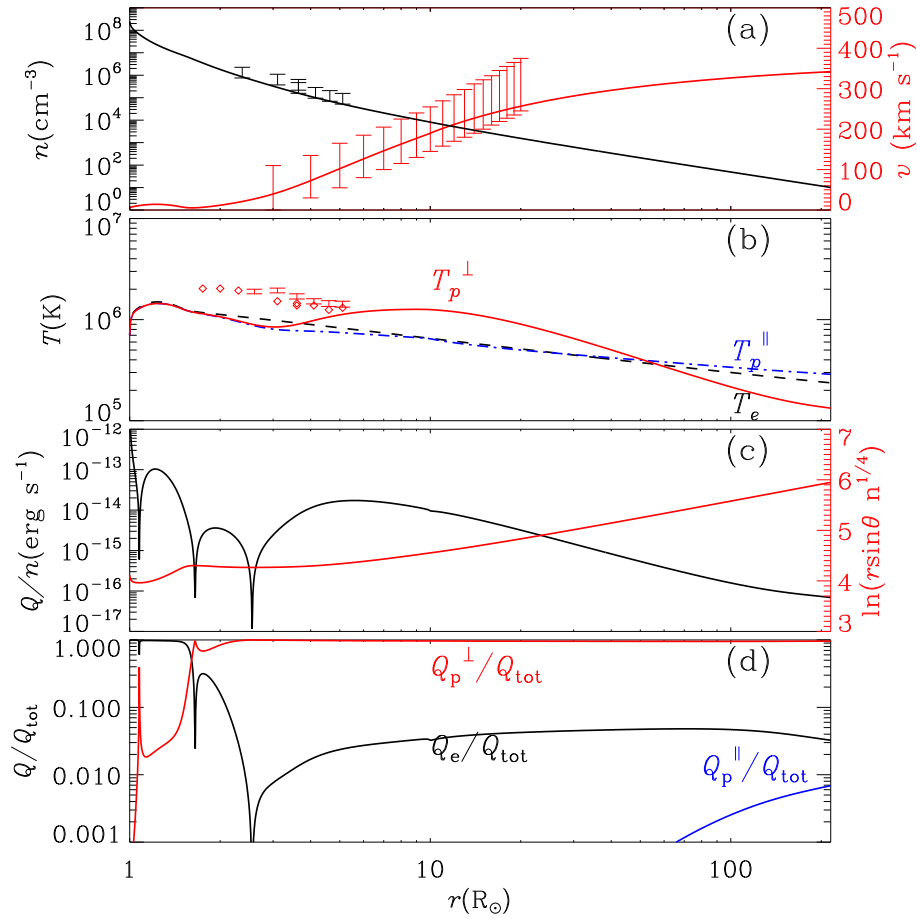


Figure 1. Radial distribution of solar wind parameters derived from an anisotropic-turbulence-heated 2-fluid model with proton temperature anisotropy. (a): number density n and speed v . (b): electron, proton parallel and perpendicular temperatures T_e , T_p^{\parallel} , and T_p^{\perp} . (c): gross turbulence dissipation rate per particle Q_{wav}/n and the geometrical factor $\ln(r \sin \theta n^{1/4})$. (d): fractions of Q_{wav} that goes to heating electrons and protons. In (a) and (b), the error bars and open boxes represent some remote-sensing measurements representative of solar minimum conditions (please see text).

Here only the outward waves contribute to the wave energy flux density F_w and wave force F , whose expressions are given by Eqs.(18) and (16) in Li et al. (1999), where the correction due to finite temperature anisotropy is included. On the other hand, the gross dissipation rate does take into account the inward waves, and the interaction between outward and inward ones yields

$$Q_{\text{wav}} = 4c_d p_w (v + v_A) \left| \left[\ln \left(r \sin \theta n^{1/4} \right) \right]' \right|, \quad (7)$$

where p_w is the wave pressure, v_A the Alfvén speed, and c_d is a dimensionless constant. Note that the field line shape appears here by contributing further reflection via the gradient of the geometrical factor $\sin \theta$. To apportion Q_{wav} among $Q_{e,\text{wav}}$ and $Q_p^{\parallel,\perp}$, Eqs.(44) to (56) in C11 are used. It suffices to mention here that a correlation scale $L_{\perp} \propto 1/\sqrt{B}$ appears not directly in Q_{wav} , as in ICW-based models (Hollweg & Isenberg 2002), but in the way Q_{wav} is apportioned.

To proceed, the field line flanking some streamer helmet is characterized by the B -distribution and its shape. These are imposed by requiring that the field line reach 88° colatitude at 1 AU in the Banaszekiewicz et al. (1998) model with their fiducial parameters (the DQCS model as presented in Fig.3 therein), and that B at 1 AU be 3.5γ . The wind is determined by the following set of parameters: the base density n_{\odot} , temperature T_{\odot} , and wave amplitude δv_{\odot} , as well as L_{\perp} at the base L_{\odot} . We choose $n_{\odot} = 2.5 \times 10^8 \text{ cm}^{-3}$, $T_{\odot} = 7 \times 10^5 \text{ K}$, $\delta v_{\odot} = 35 \text{ km s}^{-1}$, and $L_{\odot} = 100 \text{ km}$. Once these are prescribed, we first cast equations (1) to (6) in a time-dependent form and then evolve them from an arbitrary initial state until a steady state is found, which is then examined in some detail in next section.

3. Constructed slow solar wind model

Figure 1 presents the radial distribution between $1 R_{\odot}$ and 1 AU of a number of solar wind parameters. In Fig.1a, the computed number density n is compared with the electron density measurements presented in Strachan et al. (2002) (their fig.3c), while the speed profile v is compared with the range of wind speeds derived by tracking a collection of small inhomogeneities (the blobs) in images obtained with SOHO/LASCO (Wang et al. 2000). In addition to obtaining reasonable values of speed $v = 342 \text{ km s}^{-1}$ and flux density $nv = 3.5 \times 10^8 \text{ cm}^{-2} \text{ s}^{-1}$ at 1 AU, the model results agree reasonably well with the observations close to the Sun. The temperature profiles, presented in Fig.1b, are found to be difficult to reproduce the measured H I ones obtained with SOHO/UVCS and represented by the open boxes (Strachan et al. 2002) as well as error bars (Frazin et al. 2003). Despite this, the resultant pressure gradient force produces a decent slow wind solution. It is interesting to see that, the gross turbulence dissipation rate Q_{wav} exhibits multiple zeroes (Fig.1c, black curve), as a result of the geometrical factor $\ln(r \sin \theta n^{1/4})$ (Fig.1c, red curve) attaining its local extrema. This is understandable given that Q_{wav} is proportional to the gradient of this factor (Eq.7). Also noteworthy is that, among the dissipation channels of the wave energy, the Landau damping of KAWs does not make any significant contribution (Fig.1d). When the electron heating dominates ($r < 1.6 R_{\odot}$), the dissipation is due to the processes that take place at perpendicular scales shorter than the proton gyroradius. On the other hand, when the proton heating dominates ($r > 1.6 R_{\odot}$), the dissipation is almost entirely due to stochastic heating of KAWs, evidenced by the fact that protons literally receive no parallel heating. At distances

$r \gtrsim 122 R_{\odot}$ where $T_p^{\perp}/T_p^{\parallel}$ is substantially smaller than unity, the solution becomes firehose unstable. However, this should have little effect on the gross wind parameters given that the wind itself has already been fully accelerated.

4. Summary

So far the rather promising mechanism, originated by Matthaeus et al. (1999) and further developed by, to name but a few, Verdini et al. (2005); Verdini & Velli (2007); Verdini et al. (2010); Cranmer et al. (2007); Cranmer & van Ballegooijen (2012); Chandran et al. (2011), is almost entirely devoted to examining the polar fast solar wind. Does it also apply to the slow wind that flows along curved magnetic field lines bordering streamer helmets? Our preliminary results suggest that this is indeed the case.

Acknowledgments. This research is supported by the National Natural Science Foundation of China (40904047 and 41174154), the Ministry of Education of China (20110131110058 and NCET-11-0305).

References

- Banaszkiewicz, M., Axford, W. I., & McKenzie, J. F. 1998, *A&A*, 337, 940
 Chandran, B. D. G. 2010, *ApJ*, 720, 548. 1006.3473
 Chandran, B. D. G., Dennis, T. J., Quataert, E., & Bale, S. D. 2011, *ApJ*, 743, 197. 1110.3029
 Chandran, B. D. G., Li, B., Rogers, B. N., Quataert, E., & Germaschewski, K. 2010, *ApJ*, 720, 503
 Cho, J., Lazarian, A., & Vishniac, E. T. 2003, in *Turbulence and Magnetic Fields in Astrophysics*, edited by E. Falgarone, & T. Passot, vol. 614 of *Lecture Notes in Physics*, Berlin Springer Verlag, 56. arXiv:astro-ph/0205286
 Cranmer, S. R. 2002, *Space Sci.Rev.*, 101, 229
 — 2009, *Living Reviews in Solar Physics*, 6, 3. 0909.2847
 Cranmer, S. R., Panasyuk, A. V., & Kohl, J. L. 2008, *ApJ*, 678, 1480. 0802.0144
 Cranmer, S. R., & van Ballegooijen, A. A. 2012, *ApJ*, 754, 92. 1205.4613
 Cranmer, S. R., van Ballegooijen, A. A., & Edgar, R. J. 2007, *ApJS*, 171, 520. arXiv:astro-ph/0703333
 Frazin, R. A., Cranmer, S. R., & Kohl, J. L. 2003, *ApJ*, 597, 1145
 Hollweg, J. V., & Isenberg, P. A. 2002, *Journal of Geophysical Research (Space Physics)*, 107, 1147
 Li, B., & Li, X. 2009, *A&A*, 494, 361. 0812.1663
 Li, X., Habbal, S. R., Hollweg, J. V., & Esser, R. 1999, *J. Geophys. Res.*, 104, 2521
 Matthaeus, W. H., Zank, G. P., Oughton, S., Mullan, D. J., & Dmitruk, P. 1999, *ApJ*, 523, L93
 Rosner, R., Tucker, W. H., & Vaiana, G. S. 1978, *ApJ*, 220, 643
 Strachan, L., Suleiman, R., Panasyuk, A. V., Biesecker, D. A., & Kohl, J. L. 2002, *ApJ*, 571, 1008
 Verdini, A., & Velli, M. 2007, *ApJ*, 662, 669. arXiv:astro-ph/0702205
 Verdini, A., Velli, M., Matthaeus, W. H., Oughton, S., & Dmitruk, P. 2010, *ApJ*, 708, L116. 0911.5221
 Verdini, A., Velli, M., & Oughton, S. 2005, *A&A*, 444, 233
 Wang, Y.-M., Sheeley, N. R., Socker, D. G., Howard, R. A., & Rich, N. B. 2000, *J. Geophys. Res.*, 105, 25133
 Wang, Y.-M., & Sheeley, N. R., Jr. 1990, *ApJ*, 355, 726